Femtosecond phase control of spatial localization of the optical near-field in a metal nanoslit array

SooBong Choi[1], DooJae Park[1], C. Lienau[2], Mun Seok Jeong[3], Clare C. Byeon[3], Do-Kyeong Ko[3], and D. S. Kim[1*]

[1]Department of Physics and Astronomy, Seoul National University, Seoul 151-742, Korea,
[2]Institut für Physik Fk. V Carl von Ossietzky Universität Oldenburg Ammerländer Heerstraße 114-118 D-26129 Oldenburg, Germany
[3]Advanced Photonics Research Institute, GIST, Gwangju 500-712, Korea
**Corresponding author: dsk@phya.snu.ac.kr*

Abstract: We demonstrate spatial control of optical near-fields by femtosecond phase shaping in one-dimensional plasmonic structures. The near-field images display striking temporal-phase dependence, switching between double- and single-peak images within one lattice constant. The change of the near-field distribution is studied in the time and spectral domain. The spectral composition change observed by varying the time delay between two phase-locked femtosecond pulses explains the spatial control of the near-field images. Modal expansion calculations of linear light transmission using the surface impedance boundary condition are in excellent agreement with experiments.

OCIS codes: (180.4243) Microscopy; (240.6680) Surface plasmons; (320.0320) Ultrafast optics.

References and links

1. D. S. Kim, S. C. Hohng, V. Malyarchuk, Y. C. Yoon, Y. H. Ahn, K. J. Yee, J. W. Park, J. Kim, Q. H. Park, and C. Lienau, "Microscopic Origin of Surface-Plasmon Radiation in Plasmonic Band-Gap Nanostructures," Phys. Rev. Lett. **91**, 143901 (2003).
2. T. W. Ebbesen, H. J. Lezec, H. F. Ghaemi, T. Thio, and P. A. Wolff, "Extraordinary optical transmission through sub-wavelength hole arrays," Nature **391**, 667 (1998).
3. J. A. Porto, F. J. Garcia-Vidal, and J. B. Pendry, "Transmission resonances on metallic gratings with very narrow slits," Phys. Rev. Lett. **83**, 2845 (1999).
4. C. Ropers, D. J. Park, G. Stibenz, G. Steinmeyer, J. Kim, D. S. Kim, and C. Lienau, "Femtosecond light transmission and subradiant damping in Plasmonic Crystals," Phys. Rev. Lett. **94**, 113901 (2005).
5. H. F. Schouten, "Plasmon-assisted two-slit transmission: Young's experiment revisited," Phys. Rev. Lett. **94**, 053901 (2005).
6. C. H. Gan, G. Gbur, and T. D. Visser, "Surface Plasmons Modulate the Spatial Coherence of Light in Young's Interference Experiment," Phys. Rev. Lett. **98**, 043908 (2007).
7. W. L. Barnes, A. Dereux, and T. W. Ebbesen, "Surface plasmon subwavelength optics," Nature **424**, 824 (2003).
8. J. C. Weeber, Y. Lacroute, and A. Dereux, "Optical near-field distributions of surface plasmon waveguide modes," Phys. Rev. B **68**, 115401 (2003).
9. J. R. Krenn, "Non-diffraction-limited light transport by gold nanowires," Europhys. Lett. **60**, 663 (2002).
10. S. I. Bozhevolnyi, V. S. Volkov, E. Devaux, and T. W. Ebbesen, "Channel Plasmon-Polariton Guiding by Subwavelength Metal Grooves," Phys. Rev. Lett. **95**, 046802 (2005).
11. J. A. Dionne, L. A. Sweatlock, H. A. Atwater, and A. Polman, "Plasmon slot waveguides: Towards chip-scale propagation with subwavelength-scale localization," Phys. Rev. B **73**, 035407 (2006).
12. L. Yin, V. K. Vlasko-Vlasov, J. Pearson, J. M. Hiller, J. Hua, U. Welp, D. E. Brown, and C. W. Kimball, "Subwavelength Focusing and Guiding of Surface Plasmons," Nano Lett. **5**, 1399 (2005).
13. J.-C. Weeber, Y. Lacroute, A. Dereux, E. Devaux, T. Ebbesen, C. Girard, M. Ujue Gonzalez, and A.-L. Baudrion, "Near-field characterization of Bragg mirrors engraved in surface plasmon waveguides," Phys. Rev. B **70**, 235406 (2004).
14. M. I. Stockman and P. Hewageegana, "Nanolocalized Nonlinear Electron Photoemission under Coherent Control," Nano Lett. **5**, 2325 (2005).
15. M. I. Stockman, D. J. Bergman, and T. Kobayashi, "Coherent control of nanoscale localization of ultrafast optical excitation in nanosystems," Phys. Rev. B **69**, 054202 (2004).

#95545 - $15.00 USD Received 30 Apr 2008; revised 17 Jul 2008; accepted 17 Jul 2008; published 28 Jul 2008

16. M. Aeschlimann, M. Bauer, D. Bayer, T. Brixner, F. Javier Garcia de Abajo, W. Pfeiffer, M. Rohmer, C. Spindler, and F. Steeb, "Adaptive subwavelength control of nano-optical fields," Nature **446**, 301 (2007).
17. M. I. Stockman, S. V. Faleev, and D. J. Bergman, "Coherent Control of Femtosecond Energy Localization in Nanosystems," Phys. Rev. Lett. **88**, 067402 (2002).
18. A. Kubo, K. Onda, H. Petek, Z. Sun, Y. S. Jung, and H. K. Kim, "Femtosecond Imaging of Surface Plasmon Dynamics in a Nanostructured Silver Film," Nano Lett. **5**, 1123 (2005).
19. P. Anger, P. Bharadwaj, and L. Novotny, "Enhancement and Quenching of Single-Molecule Fluorescence," Phys. Rev. Lett. **96**, 113002 (2006).
20. K. Kneipp, Y. Wang, H. Kneipp, L. T. Perelman, I. Itzkan, R. R. Dasari, and M. S. Feld, "Single Molecule Detection using Surface-Enhanced Raman Scattering (SERS)," Phys. Rev. Lett. **78**, 1667 (1997).
21. H. Raether, *Surface Plasmons on Smooth and Rough surfaces and on Gratings*, (Springer-Verlag, Berlin, 1988).
22. H. Lochbihler, "Surface polaritons on gold-wire gratings," Phys. Rev. B **50**, 4795 (1994).
23. C. Genet, M. P. van Exter, and J. P. Woerdman, "Fano-type interpretation of red shifts and red tails in hole array transmission spectra," Opt. Commun. **225**, 331 (2003).
24. M. Sarrazin, J.-P. Vigneron, and J.-M. Vigoureux, "Role of wood anomalies in optical properties of thin metallic films with a bidimensional array of subwavelength holes," Phys. Rev. B **67**, 085415 (2003).
25. D. S. Yee, K. J. Yee, S. C. Hohng, D. S. Kim, T. Meier, and S. W. Koch, "Coherent Control of Absorption and Polarization Decay in a GaAs Quantum Well: Time and Spectral Domain Studies," Phys. Rev. Lett. **84**, 3474 (2000).
26. C. Obermuller and K. Karrai, "Far field characterization of diffracting circular apertures," Appl. Phys. Lett. **67**, 3408 (1995).
27. A. Kubo, Y. Suk Jung, H. Koo Kim and H. Petek, "Femtosecond microscopy of localized and propagating surface plasmons in silver gratings," J. Phys. B **40**, S259 (2007).
28. A. Kubo, N. Pontius, and H. Petek, "Femtosecond Microscopy of Surface Plasmon Polariton Wave Packet Evolution at the Silver/Vacuum Interface," Nano Lett. **7**, 470 (2007).
29. M. U. Wehner, M. H. Ulm, and M. Wegener, "Scanning interferometer stabilized by use of Pancharatnam's phase," Opt. Lett. **22**, 1455 (1997).
30. K. G. Lee, H. W. Kihm, J. E. Kihm, W. J. Choi, H. Kim, C. Ropers, D. J. Park, Y. C. Yoon, S. B. Choi, D. H. Woo, J. Kim, B. Lee, Q. H. Park, Ch Lienau, and D. S. Kim, "On the concept of imaging nanoscale vector fields," Nat. Photonics **1**, 53 (2007).
31. D. J. Park, S. B. Choi, K. J. Ahn, D. S. Kim, J. H. Kang, Q-Han Park, M. S. Jeong and D. –K. Ko, "Experimental verification of surface plasmon amplification on a metallic transmission grating," Phys. Rev. B **77**, 115451 (2008).

1. Introduction

Increasing advances in nanotechnology during the past decade have greatly improved the understanding of nano-structured metal surfaces, specifically those perforated with apertures, which possess extraordinary optical properties owing to the presence of surface plasmon polaritons excitations.[1-6] Surface plasmon polaritons (SPP) are surface-bound waves at the metal-dielectric interface, owing their existence to the surface charge density of the conductor. The surface-bound nature of SPP gives rise to the exciting possibility of overcoming the diffraction limit of light.[7, 8] For example, SPP in nano-optic systems enable one to build subwavelength scale optic circuits, which include components for propagation,[9-11] diffraction[12], and reflection,[13] etc. With integration of these nano-optic components, the issue arises how to transfer energy to a desired spatial position with subwavelength precision.

It has been theoretically explained that the spatial position of maximum field enhancement in inhomogeneous nano-systems can be controlled with chirping[15, 17] and also by varying the phase delay between two controlling femtosecond pulses.[14] Femtosecond evolution of localized hot spots and resonant surface plasmons in mesa-structured Ag gratings[18, 27, 28] and on a circular disk array[16] have been coherently controlled using the phase and polarization shape of the ultrafast excitation pulses. Though these "hot spots" have many advantages in nano-probing[19] and in sensing single molecules,[20] their inherent randomness precludes a straightforward control of nano-optical patterns formed by femtosecond laser pulses.

In this paper, we designed and studied a nano-optical model system for plasmonic femtosecond phase control, in such a way that the results are essentially understandable in an analytical way. In one-dimensional periodic nanoslit arrays, an accurate modeling of near-

#95545 - $15.00 USD Received 30 Apr 2008; revised 17 Jul 2008; accepted 17 Jul 2008; published 28 Jul 2008

field patterns, including their temporal and spectral dependencies, is possible when using a diffraction order expansion method together with the surface impedance boundary matching condition (SIBC).[3, 21, 22] We demonstrate strong variations of the near-field profile, reflecting the phase delay selective localization of SPP fields by femtosecond pulses, in close agreement with predictions from model calculations.

2. Experiments and results

2.1 On- and off-resonant SPP generations from nanoslit array

Figure 1(a) shows the studied metallic nanoslit array which has a period d=761 nm and a slit width 100 nm. 80 nm thick gold film was thermally evaporated onto a 350 μm thick sapphire substrate. Then electroresistance(ER) was spin coated about ~200nm thickness. This ER was then patterned by electron beam lithography with less than 50 nm resolution. After passing through the lithography process, patterned ER film was developed. Then the sample is milled by ion beam milling. In this process, ion beam striked gold particle only in the patterned region. After this process, the remnant ER was removed. The final array size is 100 μm X 100 μm, and the incident laser beam was not focused on the sample. The collimation of beam was seriously considered and the beam size was about 2 mm at the sample stage. This beam size was pretty much larger than the scanning area, thus we could assume that there was no spatial distortion of wavefront within scanning area. In this structure, SPP modes can be resonantly excited by TM polarized light via grating coupling at either the air-metal or sapphire-metal interfaces. The resonances are characterized by the grating momentum n**G** (n=±1, ±2, ±3, …), with G=2π/d, transferred to the incident light. The experiments reported here are performed with laser pulses centered around the lowest order AM[±1] resonance at the air-metal interface at $\lambda_{SP} = d\sqrt{\varepsilon_m/(\varepsilon_m+1)} \approx 780$ nm.[4] Here ε_m is the real part of the dielectric constant of gold.

In this case and for monochromatic light, the transmitted near-field profiles

$$I(x) \approx \int_{-\infty}^{\infty} \left| \exp(-i\omega t)\{t_0 \cdot \delta(x) + t_{+1}\exp(ik_1 x) + t_{-1}\exp(-ik_1 x)\} \right|^2 dt \,, \qquad (1)$$

are rather well described by a coherent superposition of two field contributions [23, 24]: (i) a "direct" transmission $t_0 \cdot \delta(x)$ reflecting the field transmitted through the nanoslits in the absence of SPP excitations and (ii) the "resonant" excitation of SPP fields at the air-metal interface.

#95545 - $15.00 USD Received 30 Apr 2008; revised 17 Jul 2008; accepted 17 Jul 2008; published 28 Jul 2008

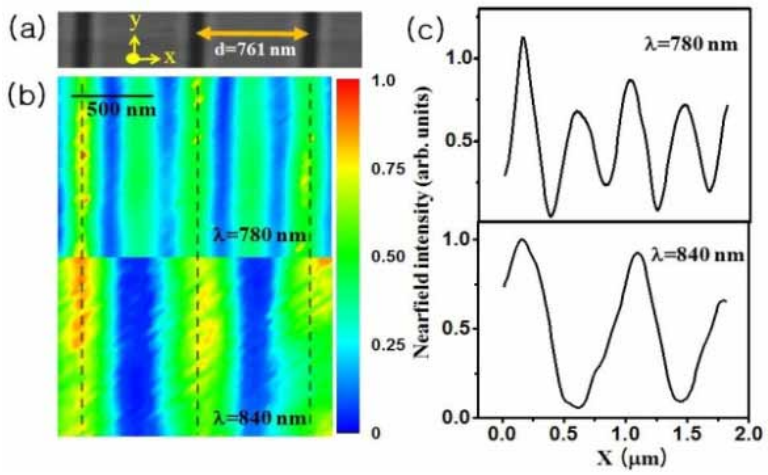

Fig. 1. (a). Scanning electron microscope image of the nanoslit array. (b) Near-field transmission images of the nanoslit array excited by monochromatic light with a wavelength of 780 nm (top) and 840 nm (bottom). The slit positions are depicted as black dashed lines in (b). (c) Cross sections of (b) showing the double periodic and the single periodic pattern within one lattice constant for excitation wavelengths of 780 nm (top) and 840 nm(bottom).

Here, the transmission coefficient t_0 describes the amplitude of the "direct" transmission and δ(x) describes the corresponding electromagnetic field localized at the slits. The coefficients $t_{\pm 1}$ describes the coupling to forward and backward propagating SPP modes, respectively. In the spectral domain, the interference between these two contributions gives rise to characteristic, asymmetric, "Fano-like" line shapes in the transmission.[23] For resonant excitation at normal incidence near 780 nm (Fig. 1(b), top), the transmission is dominated by the resonant excitation of counter-propagating SPP fields. The coupling coefficients of forward and backward propagating modes are similar $t_1 \approx t_{\pm 1}$ and the field intensity $I(x) \approx 2|t_1|^2(1+\cos(2k_1 x))$ from Eq. (1). The period of this standing wave pattern is only half of the slit period, an unambiguous signature of SPP excitation. For "off-resonant" excitation at 840 nm (Fig. 1(b), bottom), coupling to SPP modes is strongly reduced, the field intensity in between the slits vanishes and the field intensity is mainly given by the direct transmission localized at the slits $I(x) \approx 2|t_0|^2 \delta(x)^2$. These results support that near field localization at the region between slits can be selectively achieved by on- and off-resonant SPP coupling.

2.2 Time domain study of SPP generation in nanoslit array

In case of the ultrafast pulse illumination, the generated SPP retains an inherent phase from the excitation pulse. The SPP dephasing time on gold flat surface can be estimated about 150 fs in our wavelength regime [1]. According to our previous result, the dephasing time on the plasmonic structure was about 30 fs [4].This enables us to perform coherent control of the spatial images by use of two collinear pulses with a well-controlled time delay.

To control the time and phase delay between two ultrashort pulses experimentally, we adapt an actively stabilized Michelson interferometer (MI) as shown in Fig. 2. [25, 29] A continuous-wave (CW) beam from He-Ne laser (as depicted as dashed line in Fig. 2) was used for feedback and the femtosecond pulses with a center wavelength of 780 nm from

#95545 - $15.00 USD Received 30 Apr 2008; revised 17 Jul 2008; accepted 17 Jul 2008; published 28 Jul 2008

Ti:sapphire oscillator was used as the excitation light source (as depicted as solid line in Fig. 2). With external compensation using negatively chirped mirrors, about 20 fs pulse duration is achieved.

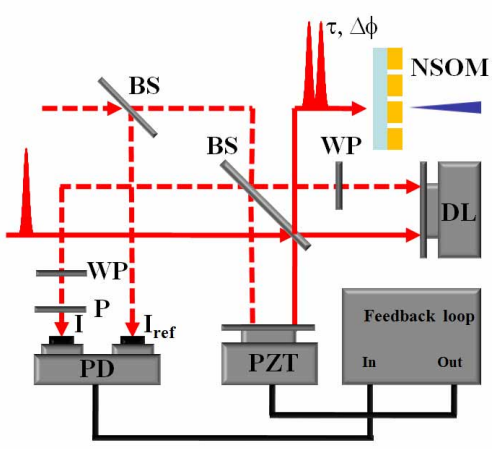

Fig. 2. Schematic diagram for actively feedback Michelson interferometer to control time delay and relative phase delay between two femtosecond pulses. WP is quarter wave plate for He:Ne laser beam, PD is photo diode, BS is 50:50 beam splitter, P is polarizer, DL is delay line, PZT is piezoelectric transducer and NSOM is near-field scanning optical microscope.

A mirror at one arm is placed on a delay line to vary the temporal separation (τ) between the two pulses. A quarter-wave plate for the CW He:Ne laser beam rotates the polarization of the beam by 90 degrees as the beam is passed through the wave plate twice. A mirror at the other arm is attached to a piezoelectric transducer without quarter-wave plate. Two orthogonally-polarized CW beams which come out of the interferometer are transmitted through another quarter-wave plate. This results in one combined CW beam with a linear polarization whose angle of polarization is determined by a relative phase between the two CW beams, that is, the minute difference between the lengths of the two arms (consequently $\Delta\tau$). The linear polarized CW beam is transmitted through a linear polarizer so that the transmitted intensity (I) is variable with the angle of the linear polarization. The signal difference between I and I_{ref} from the two photo diodes is used as a feedback signal to servo PZT in one arm for stabilization. The feedback signal is described as below:

$$I - I_{ref} = I\cos(\phi - 2\varphi + \frac{\pi}{2}) \quad , \tag{2}$$

where ϕ is a relative phase between the two CW beam and φ is a rotation angle of the polarizer. The feedback process keeps the delay $\Delta\tau$ constant within 50 attosecond. When the polarizer rotational angle is changed by $\Delta\varphi$, the relative phase delay is changed by $\Delta\phi=2\Delta\varphi$.

With the help of CW stabilization of Michelson interferometer, the femtosecond pulse splits into two collinear pulses of which time delay is τ. In the time domain, the intensity is:

$$T_E(t) = \left|\exp(-i\omega_0 t)E(t) + \exp(-i\omega_0(t-\tau))E(t-\tau)\right|^2, \tag{3}$$

where $E(t)$ is an envelope function and ω_0 is the angular frequency of λ_0=780 nm wavelength light. These time delayed pulses were TM polarized (E-field is perpendicular to the slit

#95545 - $15.00 USD Received 30 Apr 2008; revised 17 Jul 2008; accepted 17 Jul 2008; published 28 Jul 2008

direction) and normally incident on the nanoslit array from the substrate side as shown in Fig. 3(a). The transmitted near field intensity *I(x, y)* in the air-metal interface was recorded as a function of the tip position (x, y) by using a near-field scanning optical microscope (NSOM) with Aluminum (Al) coated aperture fiber probe (Lovalite, France).

In our experiment, the pulses were spectrally much broader than the AM[±1] resonance which allowed us to simultaneously generate on- and off-resonance SPP contributions. The time delay of τ=13.0 fs was chosen in order to reach a large contrast in the near-field images when varying the phase delay between $\Delta\phi=-\pi$ and $\Delta\phi=0$. The physical meaning of τ=13.0 fs will be given a full detail in Section 2.3. Phenomenologically, after the first pulse excites on- and off-resonant SPP coupling modes in nanoslit array, these SPP modes are interfered by the second pulse-generated SPP modes. With τ=13.0 fs and $\Delta\phi=0$ ($\Delta\tau$=0 fs), the phase of resonant SPP modes (ω_0) of the second pulse is identical to that of the first pulse. Thus the strengths of the resonant SPP modes are increased by the second pulse, which result the double periodic near-field distribution in one slit period, $I(x) \approx 2|t_1|^2(1+\cos(2k_1 x))$ as shown in Fig. 3(b). But with $\Delta\phi=-\pi$ ($\Delta\tau$=-1.3 fs) phase delay, the SPP distribution by the second pulse destructively interferes with the existing resonant SPP field because they are out of phase. Thus the strengths of resonant SPP modes are selectively suppressed by the second pulse. The resultant near-field distribution shows only the direct transmission localized at the slits $I(x) \approx 2|t_0|^2 \delta(x)^2$ in Fig. 3(c) as discussed in Section 2.1. Consequently, the change of the time delay and relative phase between the two pulses is an additional degree of control for the near-field intensity distribution of the nanoslit array.

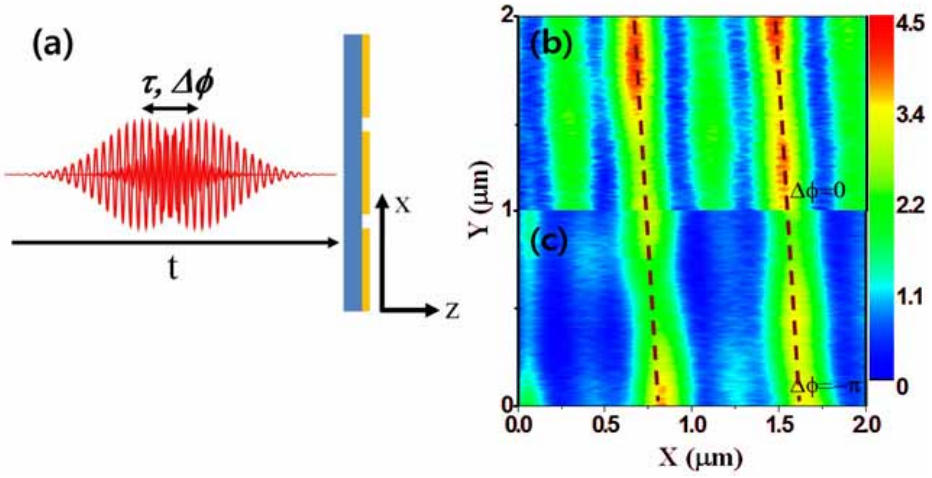

Fig. 3. (a). Phase control of spatial near field distributions by coherently controlled femtosecond pulse pairs (schematic). Near field transmission images recorded for excited by the two pulses of time delay τ=13.0 fs with (b) $\Delta\phi=0$, (c) $\Delta\phi=-\pi$, respectively. The slit positions are depicted as black dashed lines in (b) and (c).

#95545 - $15.00 USD Received 30 Apr 2008; revised 17 Jul 2008; accepted 17 Jul 2008; published 28 Jul 2008

2.3 Spectrum domain study of SPP generation in nanoslit array

The results discussed in Section 2.2 can be explained by considering the change in pulse spectrum composition upon phase variation. To build an analytical model for near field distribution in the nanoslit arrays, we assumed that the SPP generation process is essentially linear in our low intensity limit, so that Fourier analysis and modal expansion method are allowed.[31] The time-integrated spectrum of these two collinear pulses is obtained by Fourier-transforming Eq. (3) into spectrum domain and is given as

$$\left|S(\omega)\right|^2 \propto \left|E'(\omega)\right|^2\left[1+\cos((\omega-\omega_0)\tau+\phi)\right]. \quad (4)$$

Here *E'(ω)* is the Fourier transform of *E(t)* in spectrum domain and ϕ is the phase delay between the two pulses such that $\omega_0\tau=2n\pi+\phi$ where n=integer. In case of $\tau+\Delta\tau >> \Delta\tau$, τ mostly determines the period of the spectral fringes and the additional time delay $\Delta\tau=\Delta\phi/\omega_0$ (i.e. relative phase delay) does not affect the period but only shifts the peak position of the spectral fringes in Eq. (4).

Figure 4 shows that the spectrum of the incident pulses $|S(\omega)|^2$ for τ=13.0 fs, $\Delta\phi$=0 (red solid line) has a maximum at the SPP resonance (λ_0=780 nm). However, the spectrum of $\Delta\phi=-\pi$ pulses shows significant suppression around the resonant SPP wavelength (blue solid line). The time delay of τ=13.0 fs can be explained by comparing $|S(\omega)|^2$ with the spectral line width of resonant SPP coupling in nanoslit array.[1, 31]

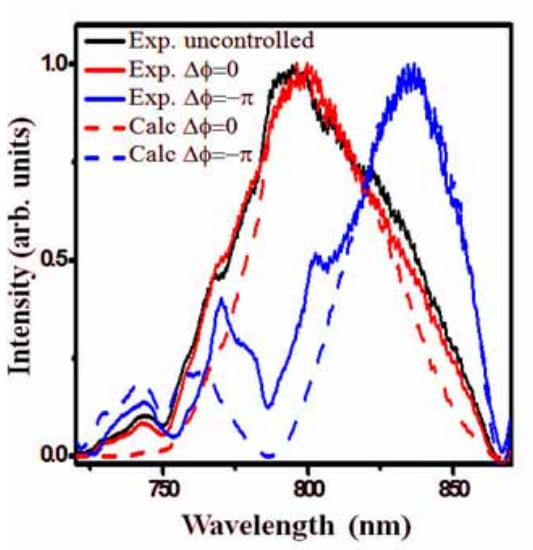

Fig. 4. The time integrated spectrum of coherently controlled incident femtosecond pulses: without phase control (black solid line), $\Delta\phi$=0 (red solid line), $\Delta\phi=-\pi$ (blue solid line) with τ= 13.0 fs. The dashed lines are simulated spectra of pulse pairs based on the uncontrolled pulse spectrum.

To consider the effect of spectral composition change on the near-field distribution more carefully, we calculated the near-field images using diffraction order expansion with SIBC. For pulsed excitation, the Fourier amplitude $t_n(\omega)$ of the n^{th} diffraction order is weighted by $S(\omega)$, so that the near field distribution is described as a function of position as:

#95545 - $15.00 USD Received 30 Apr 2008; revised 17 Jul 2008; accepted 17 Jul 2008; published 28 Jul 2008

$$I(x) = \left| \sum_{n=0}^{\infty} \int_{0}^{\infty} \{ t_n(\omega) \exp(ik_n x) + t_n(\omega) \exp(-ik_n x) \} S(\omega) d\omega \right|^2 \qquad (5)$$

To compare the simulations, which have been performed for all vector components of the electromagnetic field, to experiment, additional information about the polarization-sensitive collection properties of the aperture fiber probes is needed. It has been reported that a circularly apertured fiber tip collects the in-plane electric field component E_x perpendicular to the slit axis and magnetic field H_y along the slit axis with approximately the same efficiency.[26, 30, 31] We therefore assumed an equal coupling ratio for E_x and H_y, such that the collected intensity is proportional to $|E_x|^2 + |H_y|^2$.

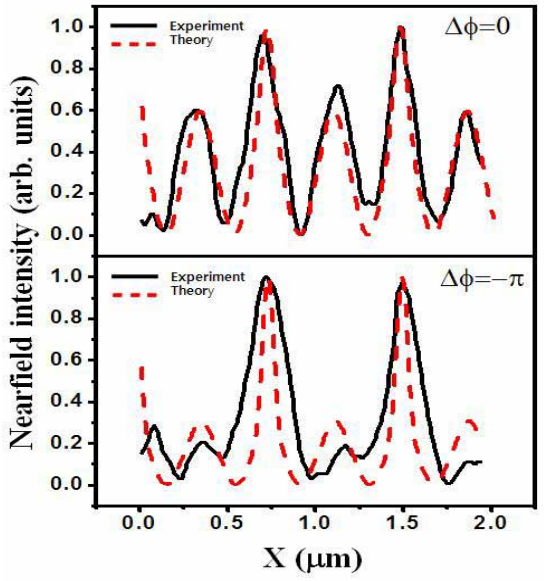

Fig. 5. Cross section intensities of Fig. 2(b), (c) (black solid lines) and theoretical simulations (red dashed lines) from the diffraction order expansion together with SIBC considering the phase-controlled variation of the pulse spectrum with time delay τ=13.0 fs (top for Δϕ=0, bottom for Δϕ=−π).

The transmitted near-field intensity *I(x)* calculated in this way is shown in Fig. 5 (top) and (bottom) as dashed red lines, together, for Δϕ=0 and -π, respectively, and is in satisfactory agreement with the experimental data (black solid lines). The phase-controlled excitation of SPP fields is clearly established and in the region between the slits the SPP field is localized to about 200 nm, which is indeed far below the diffraction limit (~400 nm) of the excitation pulses. Consequently, the control of the phase $\Delta\phi$ between the two pluses provides important additional degrees of control of the spatial distribution of the optical near-field confinement on a sub-wavelength scale.

#95545 - $15.00 USD Received 30 Apr 2008; revised 17 Jul 2008; accepted 17 Jul 2008; published 28 Jul 2008

3. Conclusion

In conclusion, we have shown that the spatial localization of the optical near field can be controlled by the varying the time delay and the relative phase between a pair of illuminating ultrashort optical pulses. In the investigated one-dimensional nano-optical system, the electromagnetic energy is localized at the desired site (here the region between the slits) with a resolution well below the diffraction limit, defined by the in-plane wavevector of the interfering SPP fields. In the present case, the temporal-phase dependent optical near-field distribution is governed by the spectrally selective coupling to SPP modes. In general, such ultrafast site selective SPP localization in a nano-system can also be achieved by chirp- or polarization-shaping of ultrafshort light pulses and is expected to find important applications in nano-optical systems, specifically in controlling energy transfer processes on the nano scale.

Acknowledgments

The authors thank Korea Government (MOST, MOEHRD) for financial support through KRF (grant number C00012 and C00032), KOSEF, Seoul R&BD program, and Nano R&D program (Grant number 2007-02939) as well as the Deutsche Forschungsgemeins for funding.

#95545 - $15.00 USD Received 30 Apr 2008; revised 17 Jul 2008; accepted 17 Jul 2008; published 28 Jul 2008